ResearchGate

See discussions, stats, and author profiles for this publication at: https://www.researchgate.net/publication/228908235

Crystal Structure of Cellulose Triacetate I

ARTICLE *in* MACROMOLECULES · JUNE 2004

Impact Factor: 5.8 · DOI: 10.1021/ma0498520

CITATIONS
19

READS
82

5 AUTHORS, INCLUDING:

Bjørn T Stokke

Norwegian University of Science and Techno…

145 PUBLICATIONS **3,718** CITATIONS

SEE PROFILE

Available from: Bjørn T Stokke
Retrieved on: 24 January 2016

Crystal Structure of Cellulose Triacetate I

Pawel Sikorski,[†] Masahisa Wada,*[,‡] Laurent Heux,[§] Hiroyuki Shintani,[‡] and Bjørn T. Stokke[†]

Department of Physics, The Norwegian University of Science and Technology, NTNU, NO-7491 Trondheim, Norway, Department of Biomaterials Science, Graduate School of Agricultural and Life Science, The University of Tokyo, Yayoi 1-1-1, Bunkyo-ku, Tokyo 113-8657, Japan, and Centre de Recherches sur les Macromolecules Vegetales (Affiliated with Joseph Fourier University of Grenoble), C.N.R.S. B.P. 53, 38401, Grenoble Cedex 9, France

Received January 22, 2004; Revised Manuscript Received April 1, 2004

ABSTRACT: Highly crystalline samples of cellulose triacetate (CTA) were prepared from cellulose I by heterogeneous acetylation in an equal amount mixture of acetic anhydride and toluene. Highly crystalline and oriented films of cellulose I from green alga *Cladophora* sp. was used as a starting material. Prepared samples were studied by FT-IR, solid-state ^{13}C NMR, and X-ray diffraction. Spectroscopic data indicate a complete degree of acetylation. In the solid-state ^{13}C NMR spectrum, each carbon atom appears only as a single resonance, indicating that the asymmetric unit in the CTA I crystal includes only a single chemical repeat unit. This behavior is in contrast with the currently accepted crystal structure of CTA I, in which the unit cell includes two parallel polymer chains. In the fiber X-ray diffraction, prepared samples show high crystallinity and good orientation. A new unit cell is proposed, and the crystalline structure was refined using molecular modeling. Possible conformations of the acetate side chains are also considered. The proposed models include a single polymer chain in a 2_1 helical conformation placed in a monoclinic unit cell with $a = 0.5939$ nm, $b = 1.1431$ nm, $c = 1.046$ nm, and $\gamma = 95.4°$. Agreement between observed and predicted diffraction intensities, compared both by visual methods and in terms of the crystallographic reliability index R, is good with $R = 0.22$.

Introduction

Cellulose triacetate (CTA) is one of the most common cellulose derivatives. In its chemical structure, all cellulose hydroxyl groups are replaced by acetyl groups. CTA has numerous applications in fiber and textile industries; it is used for membranes and films. In addition CTA has been recognized in the last few years as a powerful chiral polymeric sorbent for chromatographic separation of enantiomers.[1−3] CTA obtained from heterogeneous acetylation of microcrystalline cellulose I, investigated in this study, has the optimal properties to serve as a versatile chiral sorbent.

Depending on the nature of original cellulose samples and preparation procedures, two distinct crystal forms of the CTA can be obtained. They are referred to as CTA I and CTA II by analogy with the cellulose polymorphs: cellulose I in which chains are parallel and cellulose II in which chains are antiparallel. According to Sprague et al.[4] CTA I can only be obtained by heterogeneous acetylation of native cellulose I fibers. In the heterogeneous acetylation process the chemical reaction proceeds without dissolving the crystalline substrate, and therefore chain polarity is preserved.[4] CTA II can be prepared from cellulose II or by a homogeneous acetylation in solution of cellulose I. It was discovered[5] that CTA I can be transformed into CTA II by immersing it in some liquids that strongly swell but do not dissolve the CTA I fibers. This treatment is similar to the well-known mercerization of cellulose, where cellulose I is converted into cellulose II. There are few reports conflicting with the pioneering study of Sprague et al.[4] Watanabe et al.[6] reported that CTA I can be prepared by a heterogeneous acetylation of mercerized ramie (cellulose II). Roche et al.[7] also reported that X-ray fiber diffraction patterns of CTA I were obtained from fibers obtained from liquid crystalline solution of CTA, in which case one would expect an antiparallel CTA II form. These findings suggested that there are still some concerns regarding the chain polarity and chain organization in the CTA I crystals.

More important, in the CP/MAS ^{13}C NMR spectrum of CTA I reported recently,[8−11] and also in a high resolution spectra reported here, each of the glucose ring carbon atom shows only as a single resonance. This behavior indicated that the asymmetric unit of CTA I should in fact consist only of a single glucose unit. This conclusion is in contradiction with the currently accepted crystal structure of CTA I. This structure, proposed by Stipanovic and Sarko,[12] is based on an orthorhombic unit cell with $a = 2.363$ nm, $b = 0.627$ nm, and $c = 1.043$ nm, and the unit cell contains two parallel polymer chains.

In previous structural studies of CTA I, samples with low crystallinity prepared from ramie cellulose were used. Recently, Nishiyama et al.[13] developed a method to make uniaxial orientated films of highly crystalline cellulose microcrystals. As a consequence, we are able to use highly crystalline and well oriented cellulose I films, which are then converted into CTA I by heterogeneous acetylation. As a result, a large increase in the quality of the fiber diffraction pattern can be achieved.

* To whom correspondence should be addressed. E-mail: wadam@sbp.fp.a.u-tokyo.ac.jp.
[†] The Norwegian University of Science and Technology.
[‡] The University of Tokyo.
[§] Centre de Recherches sur les Macromolecules Vegetales (Affiliated with Joseph Fourier University of Grenoble), C.N.R.S. B.P. 53.

10.1021/ma0498520 CCC: $27.50 © 2004 American Chemical Society
Published on Web 05/20/2004

In combination with the NMR data, we are able to further refine the structure of CTA I polymorph.

Experimental Section

Cellulose Sample. A green alga *Cladophora* sp. was harvested from the Sea of Chikura, Chiba, Japan. The whole plants were immersed overnight in 5% KOH at room temperature. After thoroughly washing in water, they were then purified by bleaching in 0.3% $NaClO_2$ at 70 °C for 3 h. Treatment was repeated a few times until the sample became perfectly white.[14] The purified cell wall was homogenized into small fragments using a double-cylinder type homogenizer and lyophilized. The powder samples thus obtained were stored in a desiccator until use.

To make suspension of cellulose microcrystals dispersible in water, purified samples were treated with 50% sulfuric acid at 70 °C for 8 h with continuous stirring. The samples were then washed with deionized water by successive dilution and centrifugation at 3200*g* for 5 min until the supernatant became turbid. The suspension was concentrated by a high-speed centrifuge at 18 800*g* for 40 min and then dispersed in a small amount of distilled water. The concentrated (about 20 g/L, 50 mL) suspension was sonicated with a rod type sonicator at 20 kHz for 1 min. The suspension was cast on a glass plate and dried in air for a few days. The cast films with random orientation were further dried at 105 °C for 8 h and stored in a desiccator until use.

Oriented films of cellulose microcrystals were prepared according to the method described previously.[13] In short, the suspension with a small amount of sulfuric acid was put into a glass vial, and the vial was then kept horizontal and rotated around its center. After a few hours, the gel layer attached to the inner surface of the glass vial was dried into a film by repeated treatments of rinsing with ethanol and drying with a warm airflow. The films of oriented microcrystals were further dried at 105 °C for 8 h and stored in a desiccator until usage.

Preparation of Cellulose Triacetate I. Heterogeneous acetylation of the cellulose samples were carried out according to the method reported by VanderHart et al.[11] The dried cellulose samples were soaked in 90% acetic acid for 2 h and then in two exchanges of 100% acetic acid for 1 h each. The acetic acid wet celluloses were then immersed in an 1:1 v/v mixture of acetic anhydride and toluene with a small amount of 60% perchloric acid as a catalyst. The reaction was allowed to proceed for 20 h at room temperature. The reaction was stopped by placing the CTA samples in 95% ethanol solution for several hours. The ethanol washed samples were immersed overnight in methanol with exchanging every 2 days. After three exchanges of methanol, they were dried in air and further in vacuo at room temperature. The samples thus obtained were annealed in a nitrogen atmosphere at 240 °C for 10 min.

Acetylated cellulose was dissolved in deuterated chloroform, and analyzed by ^{1}H NMR, which gave a degree of substitution of 3.0 acetyl groups per glucose unit.

Solid-State ^{13}C NMR Spectroscopy. The acetylated cellulose was characterized by solid-state NMR. The experiments were performed with a Bruker MSL spectrometer operated at a ^{13}C frequency of 25 MHz, using the combined techniques of proton dipolar decoupling (DD), magic angle spinning (MAS), and cross-polarization (CP). ^{13}C and ^{1}H field strengths of 64 kHz corresponding to 90° pulses of 4s were used for the matched spin-lock cross-polarization transfer. The spinning was set at a rate of 3000 Hz. The contact time was 1 ms, the acquisition time 70 ms, the frequency width 29 400 Hz, and the recycling delay 4 s. Typically, 10 000 scans were acquired for each spectrum. Chemical shifts were referred to tetramethylsilane after calibration with the carbonyl signal of glycine at 176.03 ppm.

FT-IR Spectroscopy. The random oriented thin films before and after acetylation were analyzed by FT-IR spectroscopy, using a Nicolet Magna 860. The wavenumber range scanned was 4000−400 cm^{-1}; 64 scans at 4 cm^{-1} intervals were averaged and stored.

Table 1. Definition of the Torsion Angles Defining the Three Dimensional Shape of the CTA I Polymer

torsion angle	atoms			
φ	O5	C1	O4′	C4′
ψ	C1	O4′	C4′	C5′
$\chi 2$	C1	C2	O2	CA2
$\chi 3$	C4	C3	O3	CA3
$\chi 5$	C4	C5	C6	O6
$\theta 2$	C2	O2	CA2	0A2
$\theta 3$	C3	O3	CA3	OA3
$\theta 4$	C6	O6	CA6	OA6

X-ray Fiber Diffraction. X-ray fiber diagrams of cellulose triacetate were obtained from a pile of oriented microcrystals films using a vacuum camera mounted on a Rigaku RU-200BH rotating anode X-ray generator. Ni-filtered Cu Kα radiation (λ = 0.15418 nm) generated at 50 kV and 100 mA was collimated by a 0.3 mm diameter pinhole. X-ray diffraction patterns were recorded on Fuji Imaging Plates (BAS−IP SR 127), and camera length was calibrated using NaF (d = 0.23166 nm).

Model Building and Structure Refinement. The molecular mechanics package Tinker 4.0[15] was used in the structural modeling. As in similar studies published before,[16−18] the basic strategy was to determine the molecular conformation of the CTA molecule and the molecular packing arrangement within the experimental unit cell. After the initial model building stage, models were refined with a combination of energy minimization (EMin) and molecular dynamics simulations, using the MM3 force field. In addition, to test that measured unit cell parameters are sound, calculated unit cell dimensions were obtained using MD calculations performed at 298 K and in the *NPT* thermodynamic ensemble.

Torsional Angle Calculations. The potential energy profiles for side chain torsional angles were calculated using the Tinker 4.0 computer program and the MM3 force field. Three different torsion bonds (χ^2, χ^3, and χ^5, see Table 1 and Figure 1) connecting side chains to the main chain at C2, C3, and C5 positions were examined. Scans were performed by setting the torsion angle under investigation at given values between 0 and 360° in 5° steps and minimizing the energy of the system.

Analysis of the Experimental Diffraction Patterns. A set of programs dedicated to fiber diffraction and developed by the Collaborative Computational Project 13 (www.ccp13.ac.uk) was used in analyses of the experimental diffraction data. After background subtraction and transform into reciprocal space (program FTOREC), patterns were integrated using the *lsqint* program. Parameters describing the shape of the diffraction signals (relative width and degree of arcing) were also determined from the experimental X-ray diffraction patterns. They were later used to display calculated intensities in the form that can be directly compared with the experimental data.

Diffraction Pattern Simulations and Comparison with Experiment. Structure factors for the proposed model were calculated using the CNS version 1.1 crystallography and NMR package.[19] The comparison between observed and calculated diffraction data, was done in two ways. First, calculated intensities were obtained by applying appropriate fiber diffraction correction factors to the squared structure factors calculated using CNS program. Calculated intensities were then displayed using the ccp13 *lsqint* program (using the *no fit* option). Second, the crystallographic reliability index R defined by $R = \Sigma |F_{obsd} - F_{calcd}|/\Sigma F_{obsd}$ was calculated; F_{obsd} are observed and F_{calcd} are calculated structure factors.

Results and Discussion

FT-IR and ^{13}C NMR Spectroscopy. The FT-IR spectrum of CTA I is shown in Figure 2a. The bands of the OH stretching region, which are characteristic of

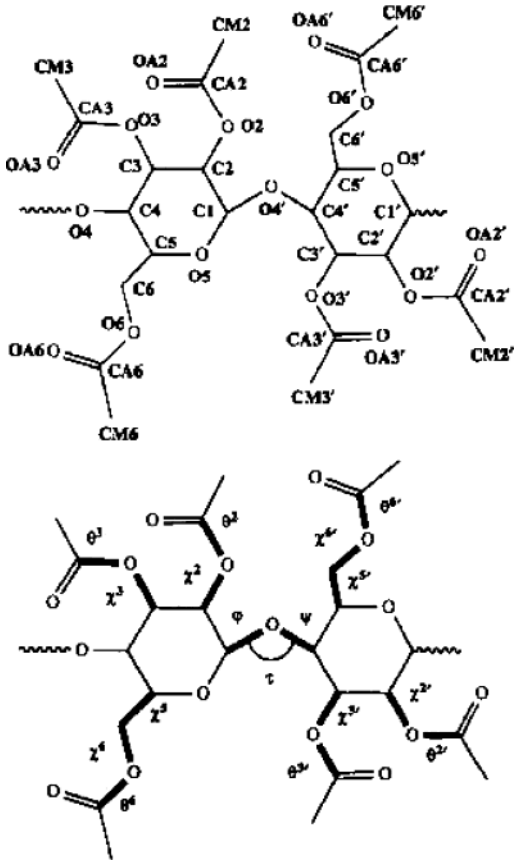

Figure 1. Atom labels and definition of the torsion angle of the CTA I repeat unit. Modified from ref 25.

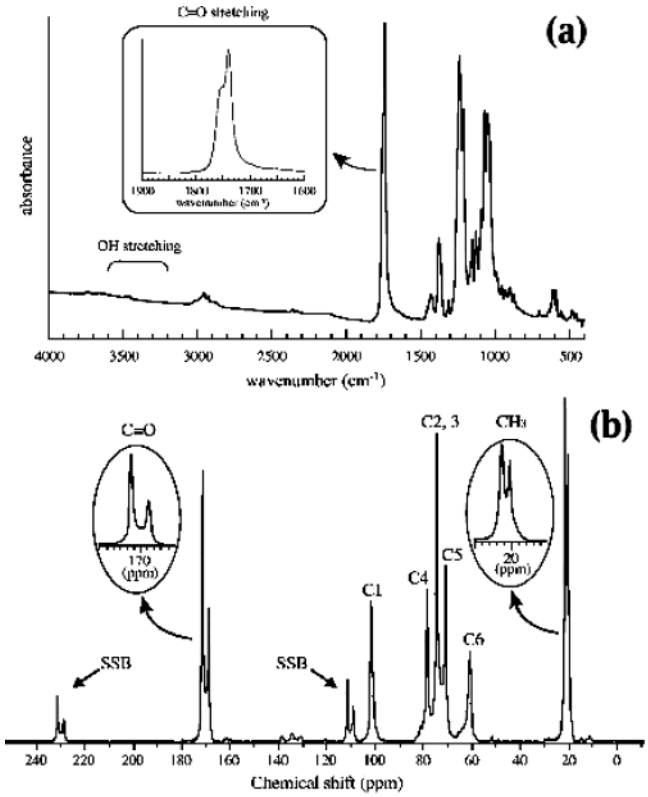

Figure 2. (a) FT-IR spectrum of CTA I. The bands of the indicated OH stretching region, characteristic of cellulose, do not appear on the spectrum. (b) Solid-state ^{13}C NMR spectrum of CTA I. See text for description. SSB indicates spinning sideband.

cellulose, located at the region 3200−3600 cm^{-1}, do not appear on the spectrum. Instead strong bands of C═O stretching are observed at 1739 and 1754 cm^{-1} (peak and shoulder). The ^{13}C NMR spectrum of the sample is shown in Figure 2b. This spectrum shows all the characteristic features of the CTA I NMR spectra reported previously, which further indicates that the starting cellulose I was fully converted to CTA I[8−11] by the employed chemical treatment.

X-ray Diffraction. The wide-angle X-ray diffraction pattern obtained with the incident beam directed orthogonal to the CTA I fibers is shown in Figure 3a. Important features of this diffraction pattern are summarized below. The CTA I sample studied is highly crystalline, with diffraction signals recorded up to (0.17 $nm)^{-1}$. In addition, no scattering from amorphous or purely oriented parts of the sample are observed, suggesting a large sample homogeneity and a high degree of crystallinity. Diffraction signals are distributed on layer lines spaced at 0.0957 nm^{-1} with observed meridional reflections on the second, fourth, and sixth layer lines. This distribution of layer line intensity suggests a 2-fold helical conformation for the CTA I molecule. The diffraction signals index on a monoclinic unit cell with the following parameters (±SD): a = 0.5939 ± 0.0011 nm, b = 1.1431 ± 0.0016 nm, c (chain axis) = 1.046 ± 0.0020 nm, and γ = 95.4 ± 0.19°. Unit cell parameters were determined using least-squares refinement method and the d-spacings of 20 strong diffraction signals listed in Table 2. The texture of the fiber diffraction pattern (c^* is orthogonal to the a^*b^* plane) indicates that both α = 90° and β = 90°. As a consequence, these two angles were kept constant in the

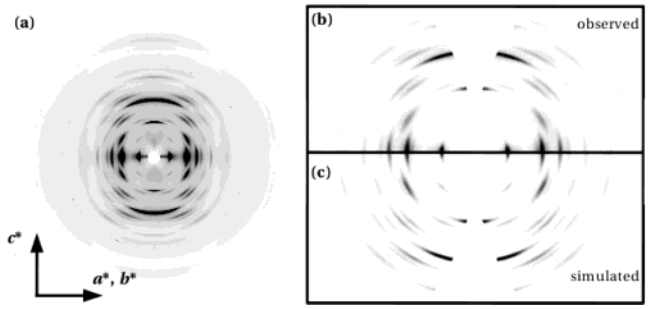

Figure 3. CTA I fiber X-ray diffraction pattern (a). Comparison between observed (b) and simulated (c) X-ray diffraction patterns for CTA I in the reciprocal space. Spacings, observed, and calculated structure factors of all diffraction signals within the resolution range covered by the experiment are listed in Table 3.

refinement of the unit cell. The agreement between observed and calculated spacings is very good, and the standard deviation of the fit is low. Density considerations suggest that the unit cell contains a single polymer chain (see below). A summary of the diffraction spacings, indexing, and relative intensities are given in Table 3. It is worth noting that this unit cell parameters are different from CTA I unit cell parameters proposed in the past.[4,12] Therefore, these previous studies will be discussed below.

Unit Cell Considerations. In the past at least two different sets of the unit cell parameters for the CTA I structure were proposed. Sprague et al.[4] proposed a monoclinic unit cell with a = 2.26 nm, b (fiber axis) = 1.05 nm, c = 1.18 nm, and β = 79°. However, it was

Table 2. Comparison between Observed (d_{obsd}) and Calculated (d_{calcd}) Spacings of the Diffraction Signals Used in the Refinement of the CTA I Unit Cell Parameters[a]

h	k	l	d_{obsd} (nm)	d_{calcd} (nm)[b]	$d_{obsd} - d_{calcd}$ (nm)
0	1	0	1.138	1.138	0.000
1	0	0	0.589	0.591	−0.002
$\underline{1}$	1	0	0.509	0.506	0.002
$\bar{1}$	2	0	0.431	0.430	0.001
$\underline{1}$	2	0	0.393	0.393	0.000
$\bar{1}$	3	0	0.333	0.333	0.000
$\underline{0}$	1	1	0.768	0.770	−0.003
$\bar{1}$	1	1	0.487	0.484	0.003
1	1	1	0.456	0.456	0.000
0	3	1	0.360	0.357	0.003
0	0	2	0.524	0.523	0.001
0	1	2	0.475	0.475	0.000
1	0	2	0.392	0.392	0.000
$\underline{1}$	1	2	0.364	0.364	0.000
$\bar{1}$	2	2	0.332	0.332	0.000
1	2	2	0.311	0.314	−0.003
0	1	3	0.335	0.333	0.001
1	0	3	0.301	0.300	0.001
1	1	3	0.286	0.287	−0.001
1	2	3	0.260	0.261	−0.001

[a] Signals with strong or medium intensity, which do not overlap with other strong diffraction signals, were included in the refinement of the unit cell parameters. [b] Calculated based on the monoclinic unit cell, with $a = 0.5939 \pm 0.0011$ nm, $b = 1.1431 \pm 0.0016$ nm, c (chain axis) $= 1.046 \pm 0.0020$ nm, and $\gamma = 95.4 \pm 0.19°$ (± SD).

noted by Stipanovic et al.,[12] that an incorrect $hkl = 003$ Miller index was assigned to a very strong diffraction signal (measured in the original work at $d = 0.35$ nm) on the third layer line of the CTA I pattern. Tilting experiments have showed that this signal is actually an off-meridional. It was indexed as $hkl = 203$ in the study of Stipanovic et al.[12] (see below), and in the unit cell proposed in this work, it is indexed as $hkl = 013$ (see Table 3).

Stipanovic et al.[12] proposed an orthorhombic unit cell with $a = 2.363$ nm, $b = 0.627$ nm and $c = 1.043$ nm. This large unit cell contains two parallel polymer chains, and it had to be used to account correctly for two medium intensity equatorial diffraction signals observed at $d = 0.8$ nm and $d = 0.61$ nm.

On the diffraction patterns analyzed here, no equatorial diffraction signals at 0.8 and 0.61 nm are observed (the closest one is at 0.591 nm). In respect to the fact that the agreement between observed spacings and relative intensities of all the other diffraction signals on our pattern and these recorded previously is good, with some confidence we can conclude that these two equatorial diffraction signals do not correspond to the CTA I structure. All the diffraction signals observed on pattern shown in Figure 3a can be indexed on a unit cell containing only single polymer chain (two saccharide units related by 2_1 symmetry). The density predicted for this new CTA I unit cell is 1.375 g cm^{-3}, 6% higher than what was found experimentally.[12]

The confidence in the fact that the CTA I unit cell contains only a single polymer chain was further reinforced by a recent NMR study, which as mentioned in the Introduction suggested that the asymmetric unit contains only a single CTA chemical unit.[20]

It is worth noting that the crystalline density predicted on the basis of the unit cell proposed by Stipanovic et al.[12] was 4% lower than the density measured experimentally (1.29 g cm^{-3}). This fact should cause some concern. Because of heterogeneity of the sample, voids between crystallites, amorphous material, etc, the experimentally determined density is usually lower than the density predicted from the volume of the unit cell. A higher measured density may be an indicator of an error in determination of the unit cell parameters.

Table 3. Observed and Calculated Structure Factors for the CTA I

h	k	l	d_{hkl} (nm)[a]	F_{calcd}	F_{obsd}
0	1	0	1.139	47	50
1	0	0	0.592	26	42
$\underline{0}$	2	0	0.569	97	82
$\bar{1}$	1	0	0.546		
$\underline{1}$	1	0	0.507	21	42
$\bar{1}$	2	0	0.430	76	63
1	2	0	0.393	34	42
$\underline{0}$	3	0	0.380	5	32
$\bar{1}$	3	0	0.333	50	42
1	3	0	0.307	5	5
$\underline{2}$	0	0	0.296	3	3
$\bar{2}$	1	0	0.293	24	18
0	4	0	0.285	21	21
$\underline{2}$	1	0	0.280	21	26
$\bar{2}$	2	0	0.273	32	37
0	0	1	1.046	0	0
0	1	1	0.770	16	18
1	0	1	0.515	13	24
$\underline{0}$	2	1	0.500	42	45
$\bar{1}$	1	1	0.484	71	53
$\underline{1}$	1	1	0.456	32	34
$\bar{1}$	2	1	0.398	5	16
1	2	1	0.368	21	16
$\underline{0}$	3	1	0.357	34	39
$\bar{1}$	3	1	0.318	16	26
1	3	1	0.295	8	18
$\underline{2}$	0	1	0.285	24	24
$\bar{2}$	1	1	0.282	5	11
0	4	1	0.275	24	18
2	1	1	0.271	39	47
0	0	2	0.523	34	32
0	1	2	0.475	24	24
1	0	2	0.392	39	39
$\underline{0}$	2	2	0.385	18	29
$\bar{1}$	1	2	0.378	11	29
$\underline{1}$	1	2	0.364	58	45
$\bar{1}$	2	2	0.332	32	37
1	2	2	0.314	18	29
0	3	2	0.307	39	47
0	0	3	0.349	0	0
0	1	3	0.333	100	87
1	0	3	0.300	66	61
$\underline{0}$	2	3	0.297	24	26
$\bar{1}$	1	3	0.294	8	21
$\underline{1}$	1	3	0.287	39	42
$\bar{1}$	2	3	0.271	29	34
1	2	3	0.261	47	39
0	0	4	0.262	16	16
0	1	4	0.255	42	58

[a] Calculated based on the monoclinic unit cell, with $a = 0.5939 \pm 0.0011$ nm, $b = 1.1431 \pm 0.0016$ nm, c (chain axis) $= 1.046 \pm 0.0020$ nm, and $\gamma = 95.4 \pm 0.19°$ (± SD).

Backbone Conformation. The evidence from the oriented X-ray diffraction patterns presented in this study and published before suggests a 2-fold helical conformation for the backbone of CTA I molecules. The measured value of the repeat along the chain axis, $c = 1.046$ nm, is only slightly larger (1%) than the repeat found for cellulose I where $c = 1.038$ nm.[21] The observed repeat is consistent with the polysaccharide backbone in an extended conformation. The values of the main chain conformation angles (φ,ψ) defined as O5−C1−O4′−C4′ and C1−O4′−C4′−H4′ respectively[22] (see Figure 1 and Table 1) are (−100°, −145°). These

Table 4. Comparison between Different Structural Parameters of the CTA I Crystalline Structure Proposed in This Study and in Some Previous Investigations

CTA I	ref	φ (deg)	ψ (deg)	a (nm)	b (nm)	c (nm)	α (deg)	β (deg)	γ (deg)	ρ (g cm^{-3})
1	this work	−100	−144.7	0.5939	1.1431	1.046	90.0	90.0	95.2	1.38
2	p{-100}[25]	−100	−150.9	0.5451	1.1622	1.045	90.1	90.1	95.63	1.45
3	p{-108}[25]	−108	−142.3	0.5151	1.2162	1.053	90.1	90.0	96.13	1.46
4	S&S[12]	−98.4	−168.4	0.627	1.1815	1.043	90.0	90.0	90.0	1.24

values are similar to values found for the middle unit of the cellotriose undecaacetate[23] where (ϕ,ψ) are (−98°, −140°), cellulose I (ϕ,ψ) = (−92°, −145°)[22] and close to the energy minimum values calculated for cellulose-like linkage at (ϕ,ψ) = (−88°, −162°).[24]

Chain Packing and Crystal Structure Refinement. An energy minimized CTA I chain was placed into the monoclinic unit cell. A starting setting angle of 45° (in the *ab*-plane, measured with the respect to *a*-axis) was chosen in order to minimize overlaps between chains from adjacent unit cells. A few other setting angles were also tried and they lead to two possible scenarios: (1) energy minimization converged to a high energy minimum, or (2) it converged to the same structure as in the case of 45° starting setting angle. Constructed starting model was subjected to refinement with a combination of energy minimization and molecular dynamics at 298 and 498 K. This modeling procedure was employed to ensure that the final model is at the global energy minimum. Note that the unit cell parameters were not refined in the simulation process, and parameters determined experimentally from X-ray fiber diffraction patterns were used in all calculations.

At this stage, we should describe one of the previous investigations of the CTA I structure in more detail. In 1992, Wolf et al.[25] performed an elaborated molecular modeling study of the crystalline packings of CTA polymer. In this work, no experimental data from CTA polymers was used and crystal structure prediction was based only on energy considerations. Computational procedure involved fixing one of the polysaccharide main chain torsion angle (φ) and optimizing all the other structural parameters, i.e., remaining torsion angles and unit cell parameters. Both parallel and antiparallel chain arrangements were considered. One aim of that study was to establish which of these two possible chain arrangements is energetically preferred. It was found that the main chain conformation has a strong influence on the chain packing and therefore on the unit cell parameters. In addition, optimized unit cell parameters were quite different from those proposed from experimental diffraction data (see Table 4). It was discovered that the lowest potential energies for the structures with parallel and antiparallel chain arrangement were similar. Thus, the preferred chain arrangement could not be deduced based on molecular modeling calculations alone. Interestingly, unit cell parameters and polysaccharide chain conformation found for one of the structures, referred to as p{-100} are similar to the parameters derived in this work (see Table 4). The chain setting angle, chain packing type and side group geometry are also similar. This structure has potential energy higher by 5.7 kcal/mol than the lowest energy structure p{-108} which displays similar molecular organization, but a slightly different chain setting angle. In addition, based on molecular modeling and contrary to the experimental evidences available at the time, Wolf et al.[25] concluded that CTA I unit cell should contain only a single polymer chain and not two chains as suggested by Stipanovic et al.[12]

Density of the p{-100} crystal is 1.45 g cm^{-3}, 5% higher than the density calculated from the unit cell parameters derived here from fiber X-ray diffraction patterns (1.38 g cm^{-3}). This is not unexpected, as energy minimization calculations used do not account for the thermal motion of the atoms in the polymer chain and therefore will lead to higher densities than what is measured at room temperature.

Table 4 summarizes main structural parameters determined in this work and these found by Wolf et al.[25] for the closest matching structure (p{-100}) and for the one with the lowest potential energy (p{-108}).

Conformation of the Side Chains. Potential energy profiles calculated for the first bond of all three side chains are shown in Figure 4. We wished to ensure that conformation of the side chains is both energetically and stereochemically feasible, i.e., that the side chain arrangement is comfortably in an energy minimum rather than being driven into particular conformation by packing of the polymer chains into the unit cell derived from the experiment. This could be the case if not all possible arrangements of the side chains were examined during the structural modeling process or the experimentally derived unit cell parameters are wrong. As mentioned above, we are mostly interested in relative orientation of the side chain with respect to the main chain. Therefore, the torsion angle of the C5−C6 bond and not C6−O6 is considered (see Figure 1). Torsion angles representing conformation of the side chains in the proposed crystal structure of the CTA I are marked with arrows (Figure 4). In all cases, the considered torsion angles are at an energy minimum. It is the global energy minimum for the C2 side chain and a local energy minimum for two remaining side chains. The energy difference between these local minima and a global minimum for each of the torsion angles is less than 1 kcal/mol. The energy profile for the C5 side chain displays two well-defined minima at +60 and −60°, with the one at +60° having the lowest energy. However, a detailed examination of the molecular model showed that if the side chain is in +60° conformation, it overlaps with the side chain of the next monomer along the polymer chain. Therefore, for the CTA polymer, only the −60° conformation is possible, and it is found in our proposed CTA I structure.

Comparison between Observed and Calculated Diffraction Intensities. After the modeling stage, structure factors F_{calcd} for the proposed structure were calculated using CNS program. These structure factors were then converted into intensities and display in the form similar to the experimental pattern using ccp13 software. A comparison between experimental (b) and calculated (c) fiber diffraction patterns is shown in Figure 3. The agreement between intensities in parts b and c is good. To confirm the quality of the match between observed and calculated intensities made visually, the crystallographic reliability index R was calcu-

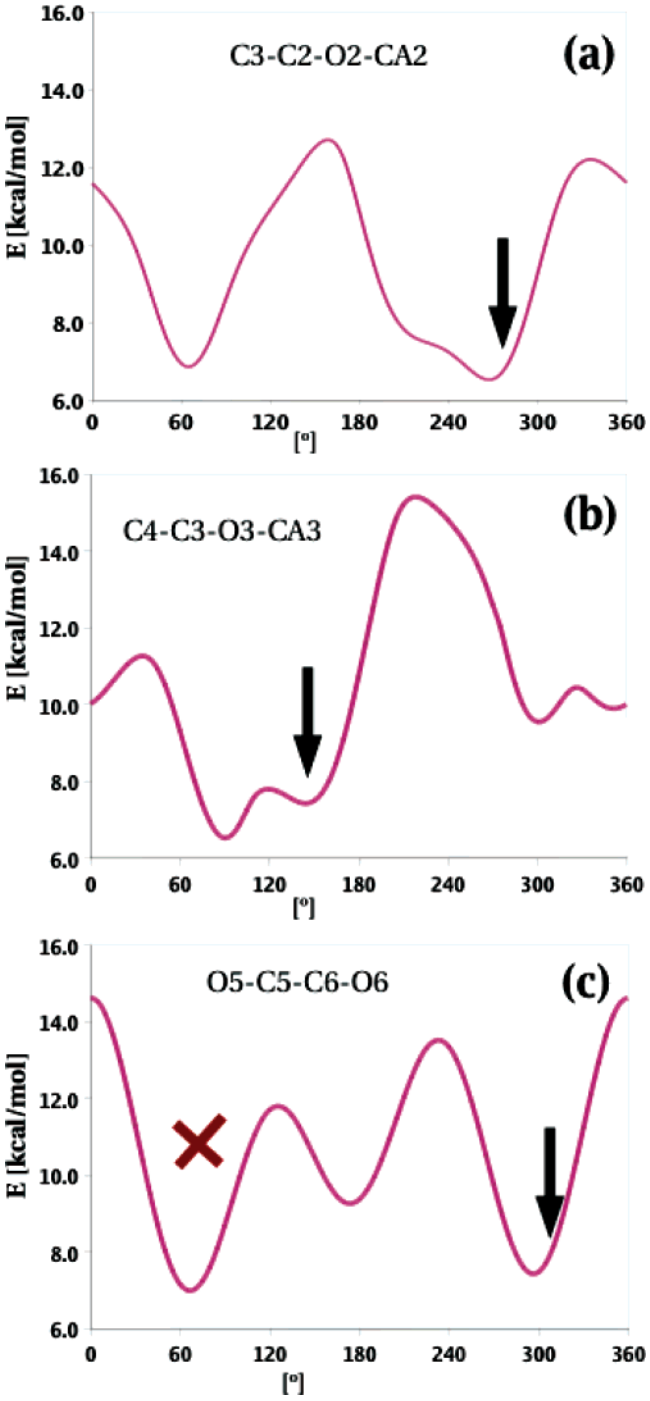

Figure 4. Potential energy profiles for the side chain torsion angles. See text for description.

lated. Its value for the model refined only by molecular modeling calculations was found to be $R = 0.224$. This low R value strongly supports the proposed structure. Because of the inaccuracy in the measured intensities and lack of data at higher resolution, further refinement would only decrease the quality of the final structure. The structure refined by molecular modeling is stereochemically sound and at the global energy minimum (within the experimental unit cell). The force field used is recognized to produce models with a high degree of similarity to structures determined from single-crystal studies.

CTA I Structure. Views of the isolated CTA chain taken from the refined model and the chains packed in the crystal structure are shown in Figure 5 and Figure

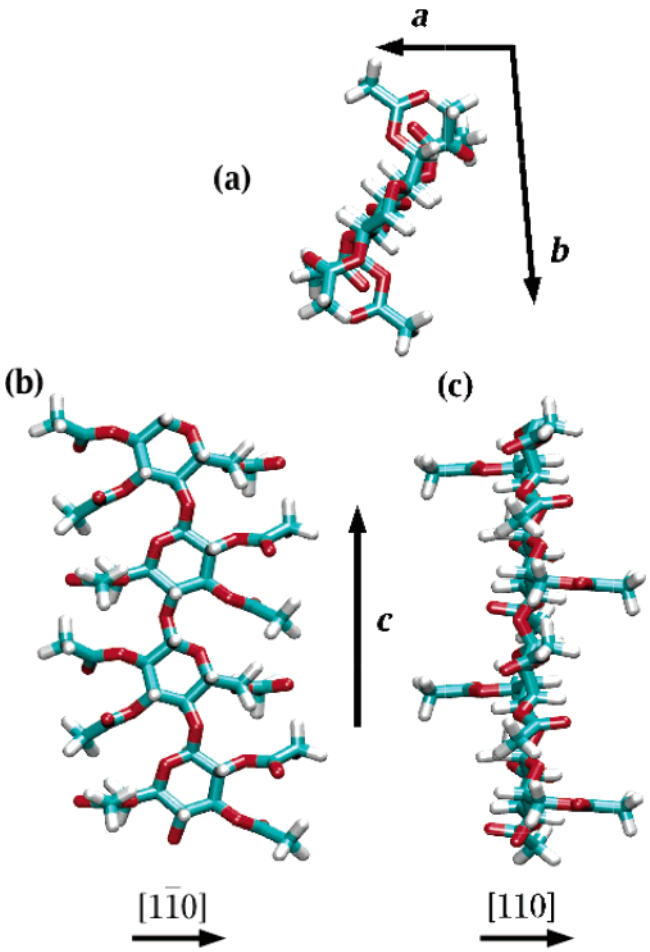

Figure 5. Three orthogonal views of the CTA I chain with the chain conformation and side chain orientations as in the final structure.

6. CTA I polymer chains in a 2_1 conformation form approximate sheets parallel to the [1$\bar{1}$0] direction (Figure 6a). The plane of the saccharide ring is parallel to the sheet plane, and the C5 side chain is oriented orthogonally to that plane. As revealed in the view of the structure parallel to the *a*-axis, packing of the side chains has a dominant influence on chain setting angle and orientation. Precise packing of the C5 side group between the C2 and C3 side chains from the molecule adjusted along the *b*-axis (circled in Figure 6b) is one of the noticeable features.

Conclusions

Highly crystalline and well-oriented cellulose I films were converted into CTA I using a heterogeneous acetylation process. As a result, highly crystalline samples of CTA I were obtained. The preparation method employed leads to a significant improvement in the quality and resolution of the experimental data recorded. CTA I samples were studied using, FT-IR, solid-state ^{13}C NMR, and X-ray fiber diffraction. Experimental data was analyzed with a help of molecular modeling. On the basis of the improved data, the crystal structure of CTA I has been refined to a considerable extent. A single polymer chain in 2_1-helical conformation is included in the monoclinic unit cell ($a = 0.5939$ nm, $b = 1.1431$ nm, c (chain axis) $= 1.046$ nm and $\gamma = 95.4°$). Agreement between observed X-ray diffraction intensities and intensities predicted from the proposed model is good, with the crystallographic reliability index $R =$

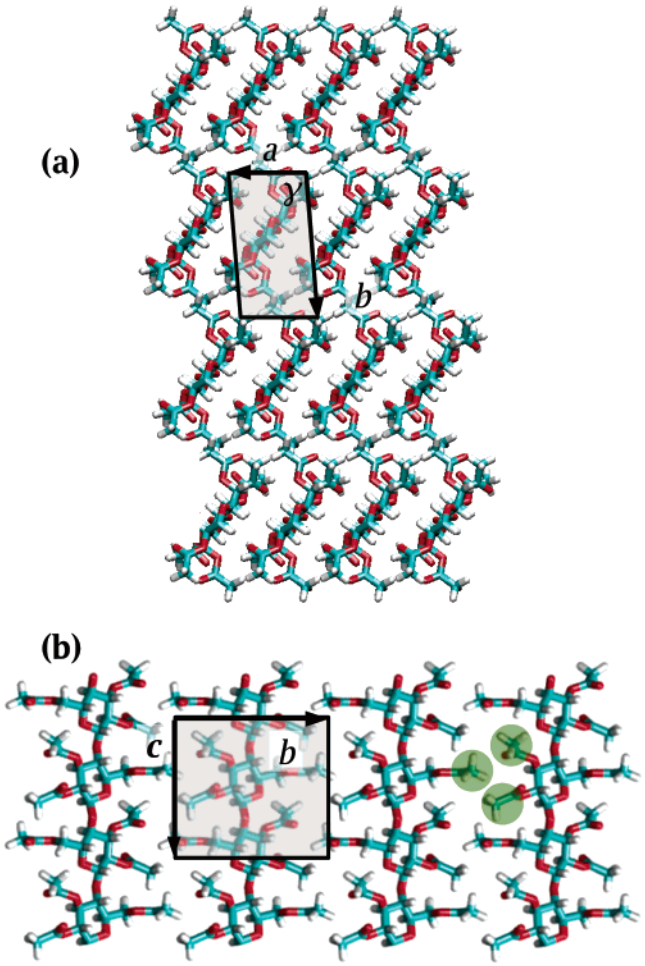

Figure 6. Views orthogonal to the *ab*- and *bc*-planes of the proposed CTA I structure.

0.224. The proposed structure provides further evidences that, similar to cellulose I, crystallites of the CTA I polymorph are composed of parallel chains.

Acknowledgment. P.S. acknowledges financial support from The Norwegian Research Council under Centre for Biopolymer Engineering at NOBIPOL, NTNU (Grant No. 145945/130). Part of this study was supported by a Grant-in-Aid for Scientific Research from the Ministry of Education, Culture, Sports, Science, and Technology, Japan.

References and Notes

(1) Hesse, G.; Hagel, R. *Liebigs Ann. Chem.* **1976**, 996.
(2) Shibata, T.; Mori, K.; Okamoto, Y. In *Chiral Separations by HPLC*; Krstulovic, A. M., Ed.; John Wiley & Sons: New York, 1989; pp 336−398.
(3) Francotte, E.; Wolf, R. M. *Chirality* **1990**, *2*, 16.
(4) Sprague, B. S.; Riley, J. L.; Noether, H. D. *Text. Res. J.* **1958**, *28*, 275.
(5) Creely, J. J.; Conrad, C. M. *Text. Res. J.* **1965**, *35*, 184.
(6) Watanabe, S.; Takai, M.; Hayashi, J. *J. Polym. Sci., Part C* **1968**, *23*, 825.
(7) Roche, E. J.; OBrien, J. P.; Allen, S. R. *Polym. Commun.* **1986**, *27*, 138.
(8) Kono, H.; Erata, T.; Takai, M. *J. Am. Chem. Soc.* **2002**, *124*, 7512.
(9) Doyle, S.; Pethrick, R. A.; Harris, R. K.; Lane, J. M.; Packer, K. J.; Heatly, F. *Polymer* **1996**, *20*, 1440.
(10) Hirai, A.; Horii, F.; Kitamaru, R. *Macromolecules* **1987**, *20*, 1440.
(11) VanderHart, D. L.; Hyatt, J. A.; Atalla, R. H.; Tirumalai, V. C. *Macromolecules* **1996**, *29*, 730.
(12) Stipanovic, A. J.; Sarko, A. *Polymer* **1978**, *19*, 3.
(13) Nishiyama, Y.; Kuga, S.; Wada, M.; Okano, T. *Macromolecules* **1997**, *30*, 6395.
(14) Sugiyama, J.; Persson, J.; Chanzy, H. *Macromolecules* **1991**, *24*, 2461.
(15) Ponder, J. TINKER−Software Tools for Molecular Design. Department of Biochemistry and Molecular Biophysics, Washington University School of Medicine: St. Louis, MO. http://dasher.wustl.edu/tinker/.
(16) Sikorski, P.; Atkins, E. D. T.; Kagumba, L.; Penelle, J. *Macromolecules* **2002**, *35*, 6975.
(17) Ehrenstein, M.; Sikorski, P.; Atkins, E.; Smith, P. *J. Polym. Sci., Part B: Polym. Phys.* **2002**, *40*, 2685.
(18) Furuhashi, Y.; Iwata, T.; Sikorski, P.; Atkins, E.; Doi, Y. *Macromolecules* **2000**, *33*, 9423.
(19) Brunger, A. T.; Adams, P. D.; Clore, G. M.; Delano, W. L.; Gros, P.; Grosse-Kunstleve, R. W.; Jiang, J. S.; Kuszewski, J.: Nilges, M.; Pannu, N. S.; Read, R. J.; Rice, L. M.; Simonson, T.; Warren, G. L. *Acta Crystallogr.* **1998**, *D54*, 905.
(20) Wada, M.; Heux, L.; Isogai, A.; Nishiyama, Y.; Chanzy, H.; Sugiyama, J. *Macromolecules* **2001**, *34*, 1237.
(21) Nishiyama, Y, Langan, P.; Chanzy, H. *J. Am. Chem. Soc.* **2002**, *124*, 9074.
(22) *Conformation of Carbohydrates*; Harwood Academic Publishers: New York, 1998.
(23) Perez, S.; Brisse, F. *Acta Crystallogr.* **1977**, *B33*, 2578.
(24) http://www.cermav.cnrs.fr/cgi-bin/di/di.cgi.
(25) Wolf, R. M.; Francotte, E.; Glasser, L.; Simon, I.; Scheraga, H. A. *Macromolecules* **1992**, *25*, 709.
(26) Some of the signals included in Table 3 have the observed intensity close to the background level. As we do not perform structural refinement based on the diffraction intensities, these signals have also been included in calculation of the *R* value. This fact can slightly increase the calculated *R* value but does not affect the quality of the refined model.

MA0498520